

BSTING: Recent progress in development of a fluid turbulence framework for stellarators

B Shanahan¹, B Dudson², and P Hill²

¹*Max-Planck Institut für Plasmaphysik, Teilinstitut Greifswald, Germany,*

²*York Plasma Institute, Department of Physics, University of York, York YO10 5DD, UK*

Introduction

The high collisionality of tokamak and stellarator edge plasmas facilitates a fluid approach to turbulence simulations. While there are several fluid turbulence simulation codes for tokamak geometries [1, 2, 3], previous attempts to develop such a simulation framework for stellarators have been unsuccessful. Here we present various new features of the BOUT++ [4] framework as part of the BSTING project – which focuses on modifying BOUT++ to allow **Simulation In Non-axisymmetric Geometries**. The BOUT++ framework is a modular, object oriented and open source framework for fluid simulations with an international team of developers [4].

The recent implementation of the Flux Coordinate Independent (FCI) [5] method for parallel derivatives in BOUT++ has allowed for simulations in non-axisymmetric geometries [6, 7]. Instead of aligning the computational grid to magnetic field lines, the FCI method uses interpolation of field line mapping on poloidal (or, in the case of linear geometries, azimuthal) planes to obtain values for finite difference differentiation. For a more complete discussion of the FCI method, see References [5, 6, 7].

Previous work in simulating non-axisymmetric geometries has focused on the conventional BOUT++ framework, which is a 3D code but was written with metric tensor components which vary in two dimensions due to an assumption of toroidal symmetry. For an accurate simulation of plasma dynamics in stellarators, BSTING must include metric components which are fully three dimensional. One major advantage of the three dimensional metrics is the ability to use a poloidal curvilinear coordinate system [8], which is described here. This newly-implemented coordinate system restores a direction of periodicity (poloidal) which allows the use of FFT-based algorithms. Furthermore, this method potentially allows for easier boundary condition implementation. While these grids have many advantages, this is the first example of a fluid turbulence code with FCI operators using a poloidally curvilinear coordinate system.

Elliptic FCI Grid generation

While all previous simulations using the FCI method have used poloidal planes with Cartesian coordinates [5, 6, 7, 3], this is not required. The method is independent of the poloidal grid

system as long as interpolation in these planes is correctly calculated and communicated. Here we present recent results using structured, non-Cartesian poloidal grids which are still logically rectangular [8]. This new grid has already been used to simulate plasma filaments in a classical stellarator geometry, a result which awaits future publication.

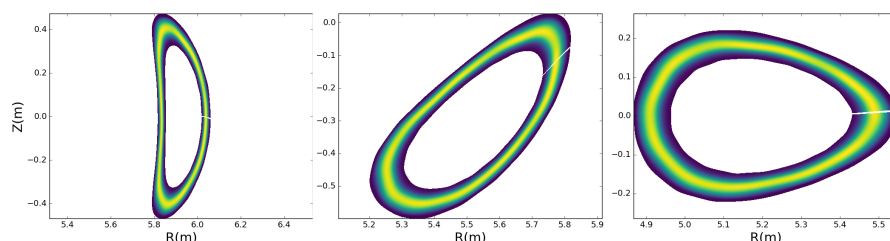


Figure 1: Three cross sections of the Wendelstein 7-X stellarator indicating flux surfaces as traced by a parallel heat diffusion equation in BSTING

These new grids have been added to the BOUT++ FCI grid generator, Zoidberg, and are included in a recent release of

BOUT++ (version 4.1).

These grids are particularly advantageous

as they include a periodic direction which could potentially increase computational efficiency. A grid is generated by prescribing an inner and outer surface, and then inverting an elliptic equation to connect the inner and outer points [8]. Both the inner and outer surface shapes are independently prescribed, and can be described using various methods: Zoidberg includes an flux surface shape generator, which will describe a shape based on elongation, triangularity and indentation. Alternatively, one can use the Zoidberg field line tracer to construct flux surfaces from a given magnetic field (i.e. from VMEC, a vacuum field solver, or an analytic magnetic field description), and generate a shape based on this flux surface. This new grid system has already been used to simulate plasma filaments in a classical stellarator geometry, a result which awaits future publication.

These grids provide an additional degree of flexibility and avoid some potential problems – primarily how to mask the core/outer edges: perpendicular (poloidal) boundaries are logically perpendicular to the grid cells, simplifying the imposition of boundary conditions – although parallel boundaries must still utilize a method such as the Leg-Value-Fill method [7] discussed earlier.

Wendelstein 7-X curvilinear grids

Here we present the development of curvilinear poloidal grids for Wendelstein 7-X [9] geometries using outputs from the VMEC code [10]. To test the implementation and limitations of grids in this complicated geometry, a diffusion model as described by Equation 1 has been implemented.

$$\frac{\partial f}{\partial t} = \nabla \cdot (\mathbf{b}\mathbf{b} \cdot \nabla f) + D\nabla \cdot (\nabla f - \mathbf{b}\mathbf{b} \cdot \nabla f) \equiv \nabla_{\parallel}^2 f + D\nabla_{\perp}^2 f \quad (1)$$

By setting the diffusion coefficient D to zero and simulating Equation 1, we can again recover flux surfaces. The results of this simulation are shown in Figure 1.

By varying the perpendicular diffusion coefficient D allows us to estimate the the inherent perpendicular diffusion in Wendelstein 7-X curvilinear grids. Figure 2 illustrates how the proportion of the test function f at the 150th timestep compares to the total test function with zero perpendicular diffusion, f_0 , for various values of D in a Wendelstein 7-X grid with a resolution of 132x16x256 (radial, toroidal, poloidal). This corresponds to a resolution of approximately 0.3mm – although this obviously is not uniform – which is a relatively coarse resolution for a Wendelstein 7-X turbulence study ($\rho_s \approx 0.1mm$).

Figure 2 indicates that the inherent numerical perpendicular diffusion caused by pollution from parallel dynamics is less than a factor of 10^{-9} times smaller than the parallel diffusion, as this is where the points begin to diverge significantly from the zero-diffusion case (as indicated by the dashed line at $f_{150}/f_0 = 1.0$). This is inherent perpendicular diffusion is sufficiently less than transport due to plasma drifts and turbulence: as stated in Reference [11], since the parallel transport is much faster than the perpendicular transport, pollution from parallel dynamics in perpendicular planes (as would appear here) must be at least 10^{-8} times smaller than the parallel transport. Should the pollution of parallel dynamics in the perpendicular plane be above this value, the resolution must be increased until this criterion is satisfied. The results presented here are encouraging as this is a moderate-resolution grid, and higher-resolution grids will most likely be necessary for future turbulence simulations in Wendelstein 7-X.

W7-X curvilinear poloidal grid for the edge and scrape-off-layer

Due to the presence of magnetic islands and stochastic fields, VMEC cannot accurately describe the magnetic field of the W7-X scrape-off-layer. To this end, development is ongoing in BSTING to generate grids based on vacuum field solvers. Figure 3 illustrates one such grid, which uses the Wendelstein 7-X web services vacuum field solver and components

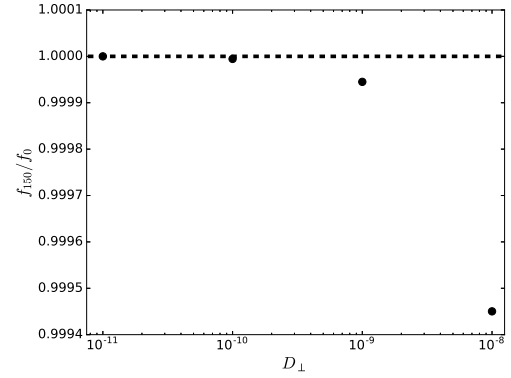


Figure 2: Proportion of the total test function f at the 150th timestep normalized to the zero-perpendicular-diffusion case, f_0 , for several perpendicular diffusion coefficients in a Wendelstein 7-X grid

database [12]. The inner surface is generated by tracing flux surfaces using a vacuum field solver, and the outer surface is generated based on a description of the Wendelstein 7-X divertor and first wall developed by Michael Drevlak for fast particle calculations, and is also available on the Wendelstein 7-X webservices [12].

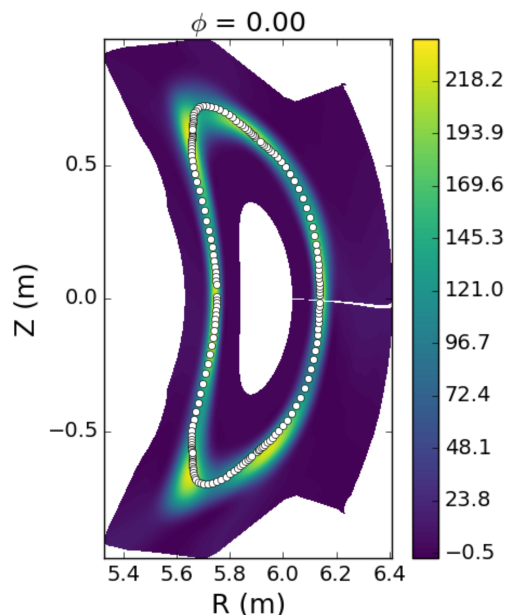


Figure 3: Simulated flux surfaces and nearby calculated Poincaré plot for the bean-shaped-cross section in a W7-X scrape-off-layer grid

Figure 3 displays the resulting flux surfaces calculated by simulating a parallel diffusion equation on the vacuum curvilinear grid. In addition to vacuum field solvers, Zoidberg has also been modified to use EXTENDER [13], allowing both plasma-generated magnetic fields and a smooth vacuum solution outside of the last closed flux surface. While a few challenges remain before full edge simulations of W7-X, this work serves as a promising first step.

Acknowledgments

The authors would like to acknowledge the work of the BOUT++ development team.

This work has been carried out within the framework of the EUROfusion Consortium and has received funding from the Euratom research and training programme 2014-2018 under grant agreement No 633053. The views and opinions expressed

herein do not necessarily reflect those of the European Commission.

References

- [1] P Ricci et al. *Plasma Physics and Controlled Fusion*, 54(12):124047, 2012.
- [2] P Tamain et al. *Contributions to Plasma Physics*, 54(4-6):555–559, 2014.
- [3] A Stegmeir et al. *Computer Physics Communications*, 198:139–153, 2016.
- [4] B D Dudson et al. *Computer Physics Communications*, 180:1467–1480, 2009.
- [5] F Hariri and M Ottaviani. *Computer Physics Communications*, 184(11):2419 – 2429, 2013.
- [6] B W Shanahan, P Hill, and B D Dudson. In *Journal of Physics: Conference Series*, volume 775, page 012012. IOP Publishing, 2016.
- [7] P Hill, B Shanahan, and B Dudson. *Computer Physics Communications*, 213:9–18, 2017.
- [8] Joe F Thompson, Zahir UA Warsi, and C Wayne Mastin. *Numerical grid generation: foundations and applications*, volume 45. North-holland Amsterdam, 1985.
- [9] C Beidler et al. *Fusion Science and Technology*, 17(1):148–168, 1990.
- [10] SP Hirshman and O Betancourt. *Journal of Computational Physics*, 96(1):99–109, 1991.
- [11] S Günter and et al. *Journal of Computational Physics*, 209(1):354–370, 2005.
- [12] SA Bozhenkov and et al. *Fusion Engineering and Design*, 88(11):2997–3006, 2013.
- [13] Michael Drevlak, D Monticello, and A Reiman. *Nuclear fusion*, 45(7):731, 2005.